

# Robust damping of interarea oscillations with unified power-flow controller

B.C. Pal

**Abstract:** An  $H_\infty$ -mixed-sensitivity design of a damping device employing a unified-power-flow controller (UPFC) is presented. The problem is posed in the linear-matrix-inequality (LMI) framework. The controller design is aimed at providing adequate damping to interarea oscillations over a range of operating conditions. The results obtained in a two-area four-machine test system are seen to be very satisfactory both in the frequency domain and through nonlinear simulations.

## 1 Introduction

The damping of interarea oscillations in power systems has been a topic of research for decades [1, 2]. The complex nature of the interactions among many control loops makes the damping-control design task challenging. The design methodology should therefore aim at improving damping performance while ensuring the least interaction with other modes over the full range of system operating conditions. This type of control action has been sought by pole-placement and eigenvalue-sensitivity-based approaches [3, 4], but these techniques do not always ensure robustness in damping performance. Additionally, the amount of control effort required in maintaining adequate damping is generally quite large.

In the last few years, the concept of  $H_\infty$  control design which can guarantee robust performance and robust stability, despite uncertainty in plant parameter variations, has been applied in power systems to damp out low-frequency oscillations [5–7]. Normally, the problem is formulated as a weighted mixed-sensitivity design and solved by a Riccati approach. The mixed-sensitivity  $H_\infty$  controller design based on the linear-matrix-inequality (LMI) formulation has shown interesting results [8] in damping-controller design since the solvability of a LMI-based formulation applies to singular plant. The numerical nature of the solution provides an improved controller with the same  $H_\infty$  norm as that obtained by the Riccati approach because the controller does not suffer from pole-zero cancellation [9]. The selection of weights has become much easier, as no restriction is imposed on the augmented plant. It is shown [10] that a controller based on an LMI approach guarantees higher damping ratios for the interarea modes than can be achieved by the controller obtained by the conventional Root-locus approach for the same control effort. The injection of real power available from a relatively small sized superconducting magnetic-energy-storage device in a controlled fashion [8, 11] has been utilised to ensure damped behaviour of power systems

following disturbances. In this paper, the same concept is extended for a UPFC.

## 2 UPFC Model

The UPFC is the most versatile FACTS device envisaged so far [12]. It offers the options of voltage regulation, phase shifting and line-impedance compensation through control of its series and shunt converters. The schematic of a UPFC connected between bus  $k$  and bus  $m$  is shown in Fig. 1. The steady-state model of a UPFC for power-flow studies has been reported in [13–15]. The simple power-injection model suggested in [14] is used here where the series- and shunt-converter voltages are replaced by nodal power injections as shown in Fig. 2. The magnitude and phase angle of the series voltage produced by the converter and the magnitude and phase angle of the AC voltage applied across the shunt converter can be controlled independently.

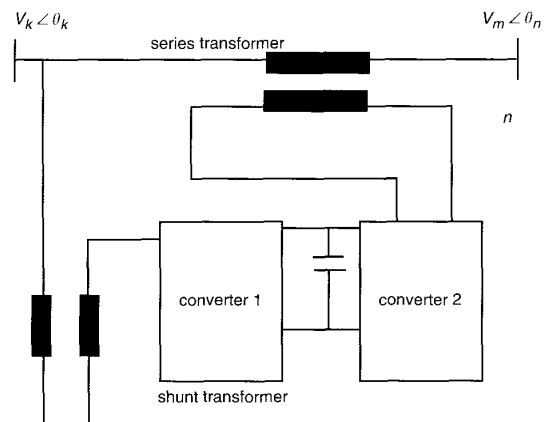


Fig. 1 Basic circuit configuration of the UPFC

In the steady state, the real power flowing through the shunt converter equals the real power exchanged between the series converter and the transmission system. This relationship puts a constraint on the independent control of the converters. Nevertheless, the reactive power of the shunt converter can be controlled independently for bus voltage

© IEE, 2002

IEE Proceedings online no. 20020660

doi:10.1049/ip-gtd:20020660

Paper first received 11th October 2001

The author is with the Control and Power Group, Department of Electrical and Electronic Engineering, Imperial College of Science, Technology and Medicine, London SW7 2BT, UK

IEE Proc.-Gener. Transm. Distrib., Vol. 149, No. 6, November 2002

733

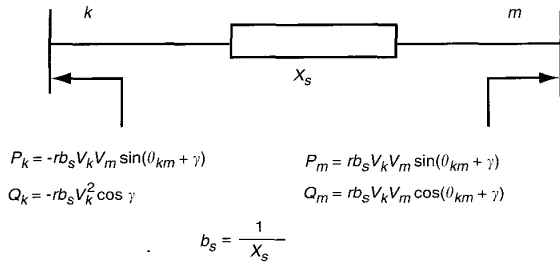


Fig. 2 UPFC power-injection model

or VAR control and the power flow through the line can be controlled through  $r$  and  $\gamma$ . For a scheduled delivery of power at the receiving end,  $r$  and  $\gamma$  will be fixed. The small-signal model is shown in Fig. 3 by two first-order blocks having small time constants of 0.02 s each. The primary purpose of the UPFC is to control power flow in the steady state. It is found in the study system that, for 400 MW and 40 MVAR to be received at bus 6, the required values for  $r$  and  $\gamma$  are  $0.10^\circ$  and  $80^\circ$ . Without UPFC, 400 MW power can be received at the cost of additional reactive-power demand at bus 6. The damping of interarea oscillations does not improve much with UPFC working on steady state. Supplementary signals are therefore necessary to damp out interarea oscillations. A power-system stabiliser (PSS) is recognised as the most cost-effective option for damping control, but with slow and DC-type excitation [16] a PSS cannot contribute much to the damping process.

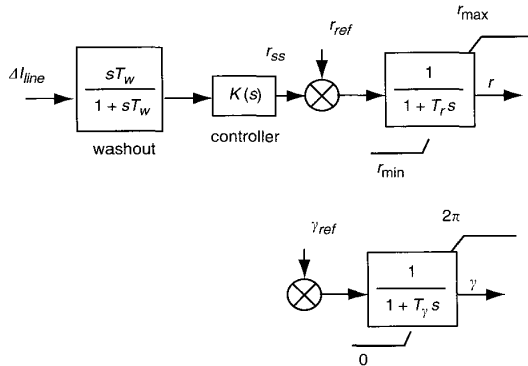


Fig. 3 Small-signal model of UPFC

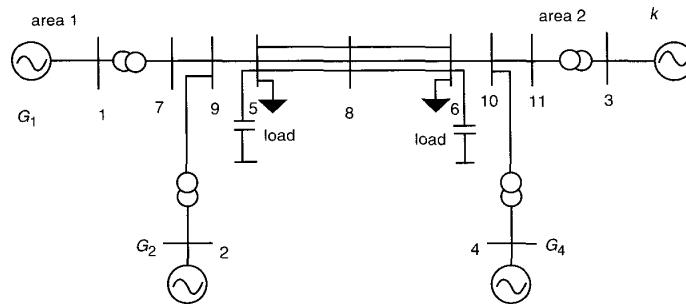


Fig. 4 Four-machine test system

In Figs. 2 and 3,  $r$  and  $\gamma$  are the UPFC variables representing the ratio of series transformer voltage to  $k$ th bus voltage in p.u. and the angle of the series voltage in radians, respectively. The term  $b_s$  is the susceptance of the series transformer combined with line susceptance  $b_{km}$ .

### 3 Study system

For study purposes, the two-area and four-machine test system shown in Fig. 4, investigated by many researchers [3, 5, 8] for interarea mode analysis, is considered. All generators are represented by three damper windings on the rotor and the excitation system is of the static DC1A type [3]. The transfer of a specified amount of power with three tielines in operation is termed the 'prefault' case. The same amount of power transfer with one of the tielines out of service is termed the 'post-fault' case. The transition from the prefault case to the post-fault case is through the opening of one of the tie circuits following a three-phase fault near bus 8 on one of the tielines. A total of 2600 MW constant-impedance (CI) load is considered at buses 5 and 6. Two capacitor banks injecting 200 MVAR each into bus 5 and bus 6 are assumed to facilitate 400 MW flow from area 1 to area 2. For this power flow, the eigenvalue analysis of the system showed three electromechanical modes with damping ratio/frequency of oscillation to be 0.08/1.08, 0.09/1.10 and 0.02/0.62 Hz respectively. The first two modes are local modes of area 1 and area 2, respectively, while the third mode involved all four machines and so is an interarea mode. The focus of this paper is on the damping-controller design for this interarea mode.

The UPFC is located in one of the circuits of the tie line with shunt converter connected to bus 5 and the series converter connected in the line between bus 5 and bus 8. Various locally available signals, e.g. bus voltage, bus frequency, real power in all the lines terminated on a bus, line-current magnitudes, rotor speed etc., are considered as the input signals. Observability analysis shows that the line real power, active line current and line-current magnitude carry valuable information about the interarea mode. The transfer function considered here is the input-output behaviour of the system between the line-current magnitude and the  $r$ -input of the UPFC. The magnitude of the line current between bus 5 and bus 9 is treated as an output signal because it has the largest observability magnitude.

### 4 LMI-based controller design

The theory of LMI detailed in [17]. The design problem treated in this paper consists of finding an internally stabilising controller that satisfies an infinity-norm

constraint. Consider the standard mixed-sensitivity configuration of Fig. 5.  $G$  is the open-loop plant,  $K$  is the controller to be designed and  $W_1$  and  $W_2$  are weights.  $y_p$  is the magnitude of the current in the line between bus 9 and bus 5.  $y$  is the deviation in line-current magnitude or error;  $w$  is the current-magnitude reference.  $z$  in Fig. 5 is an exogenous output. This design minimises a weighted mix of the transfer function  $S = (I - GK)^{-1}$  that ensures disturbance attenuation and good tracking;  $KS = K(I - GK)^{-1}$  handles the robustness issues and constrains the controller effort. This mixed-sensitivity (S/KS) design objective can be represented as

$$\left\| \begin{array}{c} W_1 S \\ W_2 K S \end{array} \right\|_{\infty} \leq \gamma$$

where  $\gamma$  is the bound on  $H_{\infty}$  norm

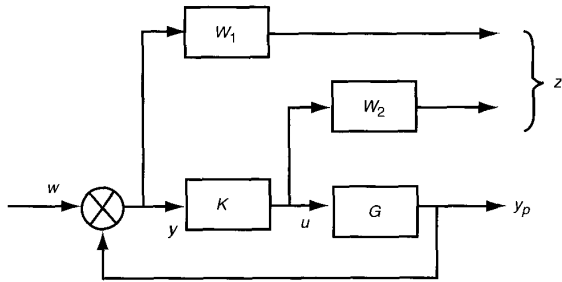


Fig. 5  $H_{\infty}$  mixed-sensitivity set-up

The details of the mixed-sensitivity control design can be found in [18]. The state-space description of the system above can be written as

$$\dot{x} = Ax + B_1 w + B_2 u \quad (1)$$

$$z = C_1 x + D_{11} w + D_{12} u \quad (2)$$

$$y = C_2 x + D_{21} w + D_{22} u \quad (3)$$

The controller  $K$  can also be described in state-space form as

$$\dot{x}_k = A_k x_k + B_k y \quad (4)$$

$$u = C_k x_k + D_k y \quad (5)$$

$D_{22}$  is dependent on the input-output relationship of the plant. For the small-signal model of the UPFC described above with line current as the stabilising feedback signal, the plant becomes strictly proper, resulting in  $D_{22} = 0$ . Other FACTS devices with a specific choice of the stabilising feedback signal may result in a nonzero  $D_{22}$ . In those cases, the design can be carried out by considering the plant as strictly proper (setting  $D_{22} = 0$ ) and the resulting controller  $K$  can be modified later to include the effect of  $D_{22}$  by putting  $\hat{K} = K(I - D_{22}K)^{-1}$ . Therefore, without loss of generality,  $D_{22}$  can be set to zero thereby making the derivation simpler.

The transfer function between  $w$  and  $z$  can be described as

$$T_{zw} = \left\| \begin{array}{c} W_1 S \\ W_2 K S \end{array} \right\| = C_{cl}(sI - A_{cl})^{-1} B_{cl} + D_{cl} \quad (6)$$

where

$$A_{cl} = \begin{bmatrix} A + B_2 D_k C_2 & B_2 C_k \\ B_k C_2 & A_k \end{bmatrix} \quad B_{cl} = \begin{bmatrix} B_1 + B_2 D_k D_{21} \\ B_k D_{21} \end{bmatrix}$$

$$C_{cl} = [C_1 + D_{12} D_k C_2, \quad D_{12} C_k]$$

$$D_{cl} = D_{11} + D_{12} D_k D_{21}$$

The objective of the mixed-sensitivity minimisation is to find an internally stabilising controller that minimises  $\left\| \begin{array}{c} W_1 S \\ W_2 K S \end{array} \right\|_{\infty}$ . In an LMI formulation [19], the same objective is achieved in the suboptimal sense if there exists an  $X = X^T > 0$  such that

$$\begin{bmatrix} A_{cl}^T X + X A_{cl} & B_{cl} & X C_{cl}^T \\ B_{cl} & -I & D_{cl} \\ C_{cl} X & D_{cl} & -\gamma^2 I \end{bmatrix} < 0 \quad (7)$$

with  $\left\| C_{cl}(sI - A_{cl})^{-1} B_{cl} + D_{cl} \right\|_{\infty} < \gamma$ ; the controller is said to be  $\gamma$  suboptimal.

The inequality in (7) contains  $A_{cl} X$ ,  $C_{cl} X$  i.e. products of  $X$  and the controller variables. The resulting problem is therefore nonlinear and so it cannot be handled directly by LMI optimisation. To make it linear, a change of controller variables is necessary. This is performed in [19, 20] and used in [8, 10] employing SMES as control device as follows.

Let  $X$  and  $X^{-1}$  be partitioned as:

$$X = \begin{bmatrix} R & M \\ M^T & * \end{bmatrix} \quad \text{and} \quad X^{-1} = \begin{bmatrix} S & N \\ N^T & * \end{bmatrix}$$

where  $R$  and  $S$  are  $n \times n$  symmetric matrices and '\*' denotes an expression not relevant for the present purpose. From the identity  $XX^{-1} = I$ , it can be inferred that  $X \begin{bmatrix} S \\ N^T \end{bmatrix} =$

$\begin{bmatrix} I \\ 0 \end{bmatrix}$  which leads to  $X \Pi_2 = \Pi_1$  with  $\Pi_1 := \begin{bmatrix} R & I \\ M^T & 0 \end{bmatrix}$ ,  $\Pi_2 := \begin{bmatrix} I & S \\ 0 & N^T \end{bmatrix}$ .

The new controller variables are defined as

$$\hat{A} = NAM^T + NB_k C_2 R + SB_2 C_k M^T \quad (8)$$

$$+ S(A + B_2 D_k C_2) R$$

$$\hat{B} = NB_k + SB_2 D_k \quad (9)$$

$$\hat{C} = C_k M^T + D_k C_2 R \quad (10)$$

$$\hat{D} = D_k \quad (11)$$

If  $M$  and  $N$  are of full row rank and if  $\hat{A}$ ,  $\hat{B}$ ,  $\hat{C}$ ,  $\hat{D}$ ,  $R$ ,  $S$  are given, the controller variables  $A_k$ ,  $B_k$ ,  $C_k$ ,  $D_k$  can be computed from (8)–(11). Moreover, if  $M$  and  $N$  are square ( $k = n$ ) and invertible matrices, then  $A_k$ ,  $B_k$ ,  $C_k$ ,  $D_k$  are unique. For full-order-controller design, it can always be assumed that  $M$  and  $N$  have full row rank; hence the variables  $A_k$ ,  $B_k$ ,  $C_k$ ,  $D_k$  can always be replaced by  $\hat{A}$ ,  $\hat{B}$ ,  $\hat{C}$ ,  $\hat{D}$  without loss of generality.

Now premultiplying and post-multiplying the inequality  $X > 0$  by  $\Pi_2^T$  and  $\Pi_2$  (7) by  $\text{diag}(\Pi_2^T, I, I)$  and  $\text{diag}(\Pi_2, I, I)$  and performing the necessary change of controller variables as defined in (8)–(11), the following simplified LMIs are

obtained [19, 20]:

$$\begin{bmatrix} R & I \\ I & S \end{bmatrix} > 0 \quad (12)$$

$$\begin{bmatrix} \Psi_{11} & \Psi_{21}^T \\ \Psi_{21} & \Psi_{22} \end{bmatrix} < 0 \quad (13)$$

The variables  $\Psi_{11}$ ,  $\Psi_{21}$  and  $\Psi_{22}$  are given in terms of new controller variables  $\hat{A}$ ,  $\hat{B}$ ,  $\hat{C}$ ,  $\hat{D}$  as

$$\Psi_{11} = \begin{bmatrix} AR + RA^T + B_2 \hat{C} + \hat{C}^T B_2^T & B_1 + B_2 \hat{D} D_{21} \\ (B_1 + B_2 \hat{D} D_{21}) & -\gamma I \end{bmatrix}$$

$$\Psi_{21} = \begin{bmatrix} \hat{A} + (A + B_2 \hat{D} C_2)^T & SB_1 + \hat{B} D_{21} \\ C_1 R + D_{12} C & D_{11} + D_{12} \hat{D} D_{21} \end{bmatrix}$$

$$\Psi_{22} = \begin{bmatrix} A^T S + SA + \hat{B} C_2 + C_2^T \hat{B}^T & (C_1 + D_{12} \hat{D} C_2)^T \\ (C_1 + D_{12} \hat{D} C_2) & -\gamma I \end{bmatrix}$$

The LMIs in (12) and (13) can be solved for  $\hat{A}$ ,  $\hat{B}$ ,  $\hat{C}$ ,  $\hat{D}$  by the recently the developed interior-point-optimisation algorithm [21]. Once  $\hat{A}$ ,  $\hat{B}$ ,  $\hat{C}$ ,  $\hat{D}$  are found, the actual controller variables  $A_k$ ,  $B_k$ ,  $C_k$ ,  $D_k$  are recovered from  $\hat{A}$ ,  $\hat{B}$ ,  $\hat{C}$ ,  $\hat{D}$  by solving (8)–(11).

The technique described above was applied to the damping-controller design for the system under study. To expedite the design process in the LMI routine [22], the plant was reduced and the controller design was then

performed on the reduced plant. The optimal Hankel-norm-approximation technique [18] was used to obtain a eight-order reduced plant by means of the Robust Control Toolbox in Matlab [23].

The standard design practice [18] in  $H_\infty$  control design is to choose  $W_1$ , as a high-gain lowpass filter for output-disturbance rejection.  $W_2$  should be a highpass filter to reduce the control effort in the high-frequency range. There should also be a lowpass filter to ensure robustness due to variation in the plant model because of varying operating conditions. There is therefore a conflict in the nature of  $W_2$  to ensure robustness and minimise control effort. The singular-value response of the weighting functions  $W_1$  and  $W_2$  are displayed in Fig. 6.

The controller was designed with the help of the Matlab LMI toolbox [22]. The controller was of 12th order, but as this large-order controller is very awkward to implement in practice, a simpler second-order controller using model reduction on the controller was obtained. The reduced second-order controller was given by

$$K(s) = -4.5 \left( \frac{s + 3.55}{s^2 + 3.38s + 3.14} \right) \quad (9)$$

## 5 Controller performance

The damping performance of the LMI controllers was examined at different operating conditions with CI loads. Table 1 shows the open-loop and closed-loop damping of three modes when 400 MW flows from area 1 to area 2. It is

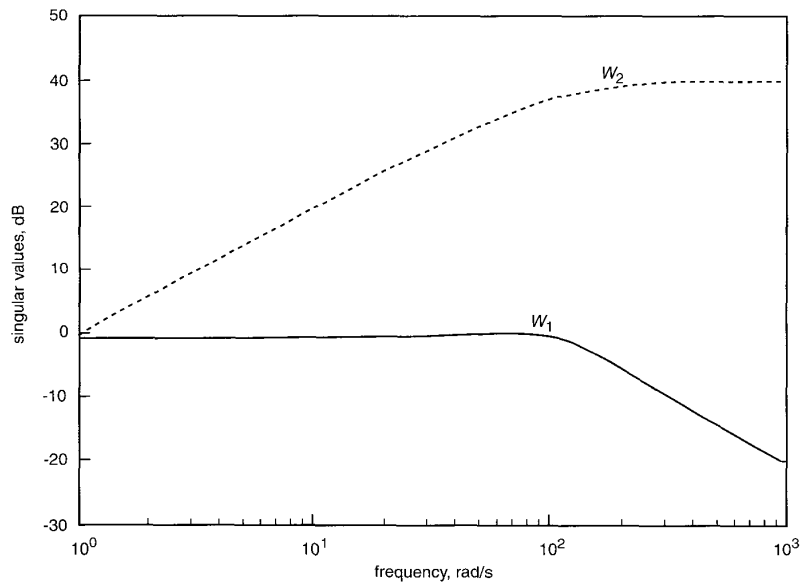


Fig. 6 Singular-value response

Table 1: Damping ratios in both operating cases

Mode	Open-loop (prefault)		Closed-loop (prefault) WNEDM-based control		Open-loop (postfault)		Closed-loop (prefault) WNEDM-based control	
	$\zeta$	$f$ (Hz)	$\zeta$	$f$ (Hz)	$\zeta$	$f$ (Hz)	$\zeta$	$f$ (Hz)
#1	0.02	0.62	0.19	0.56	0.003	0.51	0.13	0.45
#2	0.08	1.08	0.08	1.08	0.08	1.08	0.08	1.08
#3	0.09	1.10	0.10	1.10	0.09	1.10	0.10	1.10

seen from the results that the controller improves the damping of the interarea mode only. The damping of other local modes are untouched which is very desirable to avoid modal interaction through action of the controller. The damping performance of the controller was also checked at various power-flow conditions and the results are displayed in Table 2. It is found that, at different power-flow patterns, the damping is again adequate. Table 3 shows damping ratios and frequencies with constant-current (CC), constant-

**Table 2: Damping ratios at various values of power flow**

Power flow (area 1 → area 2)	Open-loop		Closed-loop	
	$\zeta$	$f$ (Hz)	$\zeta$	$f$ (Hz)
00 MW	0.02	0.65	0.20	0.64
200 MW	0.02	0.64	0.19	0.59
400 MW	0.02	0.62	0.19	0.56
-400 MW	0.02	0.60	0.12	0.58

**Table 3: Damping ratios and frequency at different load characteristics**

Load type	Interarea mode closed-loop (prefault)	
	$\zeta$	$f$ (Hz)
CI	0.19	0.56
CC	0.37	0.57
CP	0.36	0.70
CC+CP	0.27	0.54

power (CP) and an equal mix of constant-current constant-power type loads (CC+CP). From the results in Table 3, it is confirmed that the controller maintains robustness in damping to variation in load characteristics.

A nonlinear simulation was performed for a large disturbance. A three-phase fault at bus 8 was applied for 70 ms, after which the fault was cleared from the faulted line. Fig. 7 displays the large disturbance performance of the controller examined for up to 20 s. A limit of 0.10 was imposed on the controller output to restrict the series-transformer output voltage to 20% of bus 5 voltage. It is seen that the responses are very satisfactory even with system nonlinearities and the imposed operating limits of the various dynamic components.

A 16-machine 68-bus system [10] is now being investigated. The system has three interarea modes. The effect of a UPFC is being studied with other two FACTS devices: SMES and TCSC. The results will be communicated in a future paper.

## 6 Conclusions

The mixed-sensitivity-based  $H_\infty$  in the LMI framework is applied successfully in a simple two-area power system that suffers from severe interarea oscillations. A UPFC is employed as the controlling device. The performance of the controllers is seen to be robust over a range of operating conditions. The performance of the controller is found to be satisfactory at different load characteristics. The controller does not affect the damping of the other local modes. The large-disturbance performance of the controller is also seen to be very satisfactory.

## 7 Acknowledgment

The author thanks Dr. Brian Cory and Dr. Imad. M. Jaimoukha in the Control and Power Group for their comments and suggestions.

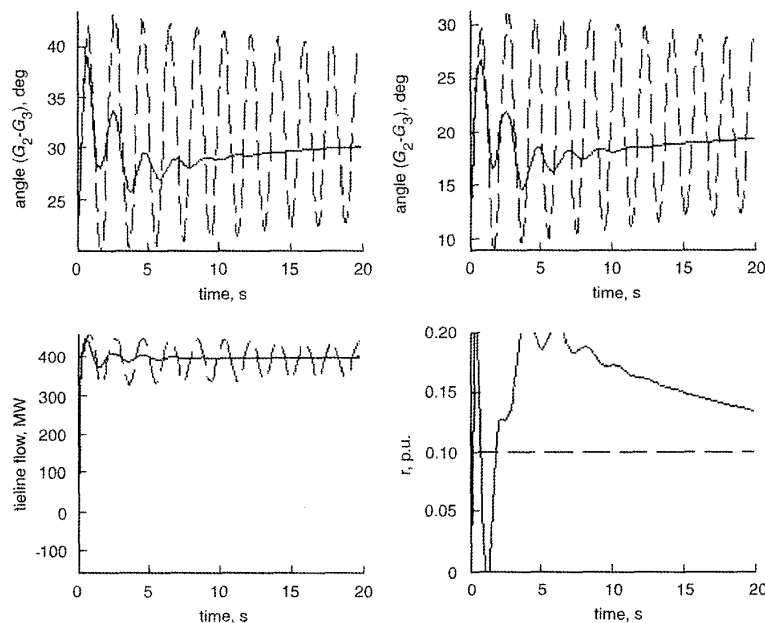


**Fig. 7** Dynamic response of the system to large disturbances

— without control  
 - - - with control

## 8 References

- 1 PASERBA, J.: 'Analysis and control of power system oscillation'. (CIGRE special publication 38.01.07) technical brochure 111, 1996
- 2 KUNDUR, P.: 'Power system stability and control', 1st edn. (McGraw Hill, USA, 1994)
- 3 KUNDUR, P., KLEIN, M., ROGERS, G.J., and ZYWNO, M.S.: 'Application of power system stabilizers for enhancement of overall system stability', *IEEE Trans. Power Syst.*, 1989, **4**, (2), pp. 614–626
- 4 ROUCO, L., PAGOLA, F.L., GARCIA-CERRADA, A., RODRIGUEZ, J.M., and SANCHEZ, R.M.: 'Damping of electromechanical oscillations in power systems with superconducting magnetic energy storage systems-location and controller design'. Proceedings of 12th Power system computation Conference, PSCC'96, Dresden, Germany, 1996, pp. 1097–1104
- 5 KLEIN, M., ROGERS, G.J., and KUNDUR, P.: 'A fundamental study of inter-area oscillations in power systems', *IEEE Trans. Power Syst.*, 1991, **6**, (3), pp. 914–921
- 6 TARANTO, G.N., and CHOW, J.H.: 'A robust frequency domain optimization technique for tuning series compensation damping controllers', *IEEE Trans. Power Syst.*, 1995, **10**, (1), pp. 1219–1225
- 7 TARANTO, G.N., SHIAU, J.K., CHOW, J.H., and OTHMAN, H.A.: 'Robust decentralised design of multiple FACTS damping controllers', *IEE Proc., Gener. Transm. Distrib.*, 1997, **144**, (1), pp. 61–67
- 8 PAL, B.C., COONICK, A.H., JAIMOUKHA, I.M., and EL-ZOBAIDI, H.: 'A linear matrix inequality approach to robust damping control design in power systems with superconducting magnetic energy storage device', *IEEE Trans. Power Syst.*, 2000, **15**, (1), pp. 356–362
- 9 SEFTON, J., and GLOVER, K.: 'Pole/zero cancellations in the general  $H_{\infty}$  problem with reference to a two block design', *Syst. Control Lett.*, 1990, **14**, pp. 295–306
- 10 PAL, B.C., COONICK, A.H., and CORY, B.J.: 'Robust damping control of inter-area oscillation with superconducting magnetic energy storage devices-an LMI approach', *IEE Proc. Gener., Transm. Distrib.*, 1999, **146**, (6), pp. 633–639
- 11 PAL, B.C.: 'Robust damping control of inter-area oscillations with superconducting magnetic energy storage devices'. PhD thesis, University of London, 1999
- 12 HINGORANI, N.G., and GYUGI, L.: 'Understanding FACTS: concepts and technology of flexible AC transmission' (IEEE Press, 2000)
- 13 NABABI-NAKIA, A., and IRAVANI, M.R.: 'Steady-state and dynamic models of unified power flow controller (UPFC) for power system studies', *IEEE Trans. Power Syst.*, 1996, **11**, (4), pp. 1937–1943
- 14 NOROOZIAN, M., ANGUIST, L., GANDHARI, M., and ANDERSON, G.: 'Use of UPFC for optimal power flow control', *IEEE Trans. Power Deliv.*, 1997, **12**, (4), pp. 1629–1634
- 15 FUERTE-ESQUIVEL, C.R., ACHA, E., and PEREZ, A.: 'A comprehensive Newton–Raphson UPFC model for the quadratic power flow solution of practical power networks', *IEEE Trans. Power Syst.*, 2000, **15**, (1), pp. 102–109
- 16 ROGERS, G.J.: 'Power system oscillations' (Kluwer Academic Press, 2000)
- 17 BOYD, S.P., GHAOUI, L., FERON, E., and BALAKRISHNAN, V.: 'Linear matrix inequalities in systems and control theory', (SIAM, Philadelphia, 1st edn. 1994)
- 18 SKOGESTAD, S., and POSTLETHWAITE, I.: 'Multivariable feedback control analysis and design', (John Wiley and Sons, 1st edn. 1996)
- 19 GAHINET, P., and APKARIAN, P.: 'A linear matrix inequality approach to  $H_{\infty}$  control', *Int. J. Robust Nonlinear Control*, 1994, **4**, pp. 421–448
- 20 CHILALI, M., and GAHINET, P.: ' $H_{\infty}$  Design with pole placement constraints: an LMI approach', *IEEE Trans., Autom. Control*, 1996, **41**, (3), pp. 358–367
- 21 NESTEROV, Y., and NEMIROVSKI, A.: 'Interior point polynomial methods in convex programming: theory and applications', (SIAM, 1994)
- 22 GAHINET, P., NEMIROVSKI, A., LAUB, A.J., and CHILALI, M.: 'LMI control toolbox for use with Matlab', (The Math Works Inc., USA, 1st edn. 1995)
- 23 CHIANG, R.Y., and SOFONOV, M.G.: 'Robust control toolbox for use with Matlab', (The Math Works Inc., USA, 1st edn. 1995)